第 33 卷第 11 期
2017 年 11 月

无 机 化 学 学 报
CHINESE JOURNAL OF INORGANIC CHEMISTRY

Vol.33 No.11
2103-2109

双核钌-DMBA 双芳香炔化合物的合成和电化学性质

Susannah D. Banziger　Eileen C. Judkins　Matthias Zeller　任　彤*
(Department of Chemistry, Purdue University, West Lafayette, Indiana 47907, USA)

摘要：在弱碱性条件下，双核钌(Ⅲ)配合物 $Ru_2(DMBA)_4(NO_3)_2$(DMBA=tetrakis-*N*,*N*′-dimethylbenzamidinate)与不同芳香炔反应(其中芳香基团包括：NAP^{me}，*N*-甲基-1,8-萘二甲酰亚胺；NAP^{iso}，*N*-异丙基-1,8-萘二甲酰亚胺；Naphth，萘；Ant，蒽)，制备了相应的端基炔取代配合物 *trans*-$Ru_2(DMBA)_4(C_2Ar)_2$(Ar=NAP^{me}，**1**；NAP^{iso}，**2**；Naphth，**3**；Ant，**4**)。利用 X 射线晶体衍射测定了它们的结构。所有化合物的 Ru-Ru 键长处于单键范围(0.245 0~0.249 1 nm)，它们均是抗磁性物质。进一步通过 ^{1}H NMR 和 UV-Vis-NIR 光谱进行了表征。电化学研究表明，所有化合物显示出与芳香基团有关的 2 个可逆的单电子氧化还原过程(包括一个氧化过程和一个还原过程)。

关键词：双核钌；炔基；1,8-萘二甲酰亚胺；萘基；蒽基
中图分类号：O614.82$^+$1　　**文献标识码**：A　　**文章编号**：1001-4861(2017)11-2103-07
DOI：10.11862/CJIC.2017.238

Diruthenium-DMBA Bis-Alkynyl Compounds with Hetero- and Extended-Aryl Appendant: Preparation and Electrochemical Property

Susannah D. Banziger　Eileen C. Judkins　Matthias Zeller　Tong Ren*
(*Department of Chemistry, Purdue University, West Lafayette, Indiana* 47907, *USA*)

Abstract: Under weak base conditions, diruthenium(Ⅲ) tetrakis-*N*,*N*′-dimethylbenzamidinate (DMBA) nitrate $Ru_2(DMBA)_4(NO_3)_2$ was reacted with arylethyne ligands, where aryl=NAP^{me} (*N*-methyl-1,8-naphthalimide), NAP^{iso} (*N*-isopropyl-1,8-naphthalimide), Naphth (naphthalene) and Ant (anthracene), to afford four new compounds: *trans*-$Ru_2(DMBA)_4(C_2Ar)_2$ (Ar=NAP^{me}, **1**; NAP^{iso}, **2**; Naphth, **3**; Ant, **4**). Molecular structures of new compounds were determined using single crystal X-ray diffraction, and the Ru-Ru bond lengths (0.245 0~0.249 1 nm) are consistent with the existence of a Ru-Ru single bond. These compounds are diamagnetic and were further characterized with ^{1}H NMR and UV-Vis-NIR spectroscopic techniques. Cyclic voltammograms of compounds **1**~**4** consist of two reversible one-electron processes, an oxidation and a reduction, and their potentials depend on the nature of Ar. CCDC 1555598, **1**; 1555599, **2**; 1555609, **3**; 1555611, **4**.

Keywords: diruthenium; alkynyl; naphthalimide; naphthalene; anthracene

0 Introduction

Conjugated metal-alkynyl compounds are of interest to both the inorganic and materials chemistry communities[1-3] and have been studied as prototypical molecular wires[4-7], light emitting materials[8-9] and photovoltaic materials[10]. Recent interesting examples of linearly conjugated metal alkynyl or metal alkenyl species include those based on mono- and bimetallic Ru compounds supported by phosphine[11-14] and $PtAu_2$

收稿日期：2017-06-14。收修改稿日期：2017-08-23。
美国国家科学基金会(No.CHE 1362214，CHE 1625543)资助项目。
*通信联系人。E-mail：tren@purdue.edu

heterometallics[15-16].

Diruthenium compounds bearing axial alkynyl ligands are known for their capacity to undergo multiple reversible one-electron oxidation/reduction[2], strongly couple across oligoyn-diyl bridges[17-19], mediate couplings between two ferrocenyls[20], facilitate the formation of supramolecules[21-22], and function as the active species in molecular devices[23-24]. Among *N*,*N*′-bidentate ligands used to support the Ru_2 core, DMBA (*N*,*N*′-dimethylbenzamidinate) and its derivatives are the most electron donating and support a variety of Ru_2(Ⅲ, Ⅲ) bis-alkynyls[25-27] and Fe-Ru_2 heterometallic complexes[28]. Reported in this contribution are four new *trans*-$Ru_2(DMBA)_4(C_2Ar)_2$ type compounds with Ar as 4-*N*-methyl-1,8-naphthalimide (**1**), 4-*N*-isopropyl-1,8-naphthalimide (**2**), 1-naphthalene (**3**) and 9-anthracene (**4**), as sketched in Scheme 1.

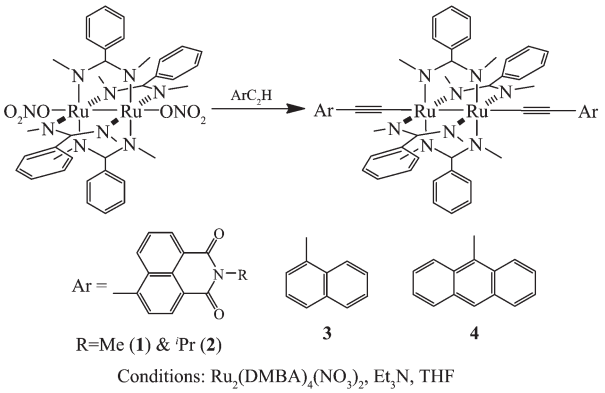

Scheme 1 New $Ru_2(DMBA)_4(C_2Ar)_2$ compounds

1 Experimental

1.1 Materials and measurements

$[Ru_2(DMBA)_4(NO_3)]$ was prepared according to literature procedures[29]. Also prepared according literature procedures were 1-ethynylnaphthalene[30], 9-ethynylanthracene[31], and 4-ethynyl-*N*-methyl-1,8-naphthalimide[32]. THF was distilled over Na/benzophenone under a N_2 atmosphere. Diisopropylamine was purchased from Acros Organics and distilled over potassium hydroxide. The synthesis of Ru_2 compounds was performed under ambient atmosphere. All other reactions were carried out using Schlenk techniques under N_2. UV-Vis-NIR spectra were obtained with a JASCO V-670 UV-Vis-NIR spectrophotometer. Infrared spectra were obtained on a JASCO FT-IR 6300 spectrometer via ATR on a ZnSe crystal. ^{1}H NMR spectra were recorded on a Varian MERCURY300 NMR. Cyclic voltammograms were recorded in 0.1 mol·L^{-1} *n*-Bu_4NPF_6 and 1.0 mmol·L^{-1} ruthenium species solution (THF, Ar degassed) using a CHI620A voltammetric analyzer with a glassy carbon working electrode (Diameter=2 mm), Pt-wire counter electrode, and an Ag/AgCl reference electrode with ferrocene used as an internal reference.

1.2 Preparation of 4-Ethynyl-*N*-isopropyl-1,8-naphthalimide and its precursors

4-Bromo-1,8-naphthalic anhydride (1.00 g, 3.61 mmol) and isopropylamine (1.00 mL, 11.66 mmol) were added to degassed ethanol (30 mL). The mixture was refluxed under nitrogen for 18 hours to yield a dark yellow solution and then placed in an ice bath. A light yellow precipitate formed which was then filtered, and rinsed with methanol (30 mL) to afford 0.89 g of 4-bromo-*N*-isopropyl-1,8-naphthalimide (77% based on 4-bromo-1,8-naphthalic anhydride). ^{1}H NMR (CD_3OD): δ 8.64 (dd, *J*=7.3, 1.1 Hz, 1H), 8.55 (dd, *J*=8.5, 1.1 Hz, 1H), 8.40 (d, *J*=7.9 Hz, 1H), 8.03 (d, *J*=7.9 Hz, 1H), 7.84 (dd, *J*=8.5, 7.4 Hz, 1H), 5.42 (hept, *J*=7.0 Hz, 1H), 1.60 (d, *J*=7.0 Hz, 6H). IR (cm^{-1}): C=O: 1 656 (s), 1 700 (s).

4-Bromo-*N*-isopropyl-1,8-naphthalimide (890 mg, 2.80 mmol), $Pd(PPh_3)_2Cl_2$ (40 mg, 0.057 mmol) and CuI (11 mg, 0.058 mmol) were dried under vacuum for 3 hours, upon which 35 mL of diisopropylamine and ethynyltrimethylsilane (0.8 mL, 5.78 mmol) were added. The dark brown solution was allowed to stir at room temperature for 30 minutes and then heated to reflux for 30 minutes until the solvent became black. Upon rotary evaporation, the off-white solid was redissolved in EtOAc, rinsed through a short silica plug, and purified by column chromatography (SiO_2, $V_{CH_2Cl_2}/V_{hexanes}$=1) to afford 855 mg of 4-ethynyltrimethylsilyl-*N*-isopropyl-1,8-naphthalimide (91% based on 4-bromo-*N*-isopropyl-1,8-naphthalimide). Desilylation of 4-ethynyltrimethylsilyl-*N*-isopropyl-1, 8-naphthalimide (675 mg, 2.01 mmol) was accomplished using K_2CO_3 in a MeOH/CH_2Cl_2 (2∶1, *V*/*V*) solution to afford 524

mg of 4-ethynyl-*N*-isopropyl-1,8-naphthalimide (98%). ^{1}H NMR (CD_3OD): δ 8.63 (dd, *J*=8.6 Hz, 2H), 8.51 (d, *J*=7.5 Hz, 1H), 7.93 (d, *J*=7.7 Hz, 1H), 7.82 (t, *J*=7.9 Hz, 1H), 5.43 (hept, 1H), 3.72 (s, 1H), 1.60 (dd, *J*=7.0, 0.6 Hz, 6H). Visible spectra, λ_{max} / nm (ε / (L·mol^{-1}·cm^{-1})): 350 (35 240), 366 (32 580). IR (cm^{-1}): C=O: 1 653 (s), 1 700 (s); C≡C: 2 102 (m); C≡C-H: 3 227 (s).

1.3 Preparation of 1

$Ru_2(DMBA)_4(NO_3)_2$ (45.2 mg, 0.049 mmol), 4-ethynyl-*N*-methyl-1,8-naphthalimide (70.1 mg, 0.298 mmol), and Et_3N (0.6 mL) were dissolved in 50 mL THF and reacted for 4 h to yield a dark red solution. Upon solvent removal, the residue was purified by column chromatography (SiO_2, $V_{hexanes}/V_{THF}$=9). Unreacted ligand eluted first, followed closely by the desired product as a deep red band. Upon solvent removal, the red fraction was recrystallized from hexanes-THF to afford 43.7 mg of **1** (70% based on Ru). ESI-MS(*m/z*): [M]$^+$, 1 260.0. ^{1}H NMR (CD_3OD): δ 8.82 (d, *J*=8.2 Hz, 2H), 8.54 (d, *J*=7.4 Hz, 2H), 8.43 (d, *J*=7.8 Hz, 2H), 7.60 (d, *J*=7.8 Hz, 2H), 7.53~7.46 (m, 12H), 7.41 (d, *J*=7.8 Hz, 2H), 7.07 (d, *J*=7.1 Hz, 8H), 3.53 (s, 6H), 3.40 (s, 24H). Visible spectra, λ_{max} / nm (ε / (L·mol^{-1}·cm^{-1})): 322 (16 160), 460 (15 200), 550 (28 200), 877 (1 690). IR (cm^{-1}): C=O: 1 654 (s), 1 691 (s); C≡C: 2 047 (s). Anal. Found (Calcd.) for $C_{70}H_{68}N_{10}O_5Ru_2$ (**1**·THF, %): C, 63.28 (63.14); H, 5.04 (5.14); N, 10.52 (10.52).

1.4 Preparation of 2

$Ru_2(DMBA)_4(NO_3)_2$ (93 mg, 0.102 mmol), 4-ethynyl-*N*-isopropyl-1,8-naphthalimide (134 mg, 0.508 mmol) and Et_3N (0.3 mL) were reacted in 100 mL of THF for 3 h. The reaction mixture was purified similarly to that of **1** to afford 112 mg of **2** (84% based on Ru). ESI-MS(m/z): [M]$^+$, 1 316.1. ^{1}H NMR (CD_3OD): δ 8.78 (dd, *J*=8.3, 1.3 Hz, 2H), 8.50 (dt, *J*=7.3, 1.6 Hz, 2H), 8.40 (dd, *J*=7.8, 1.8 Hz, 2H), 7.74~7.27 (m, 16H), 7.10~7.02 (m, 8H), 5.47~5.34 (m, 2H), 3.40 (d, *J*=1.8 Hz, 24H), 1.57 (dd, *J*=3.1, 1.9 Hz, 12H). Visible spectra, λ_{max} / nm (ε / (L·mol^{-1}·cm^{-1})): 323 (20 940), 462 (20 050), 549 (37 140), 870 (2 450). IR (cm^{-1}): C=O: 1 653 (s), 1 690 (s); C≡C: 2 049 (s). Anal. Found (Calcd.) for $C_{74}H_{80}N_{10}O_7Ru_2$ (**2**·THF·2H_2O, %): C, 62.31 (62.43); H, 5.40 (5.66); N, 9.82 (9.83).

1.5 Preparation of 3

$Ru_2(DMBA)_4(NO_3)_2$ (0.095 g, 0.104 mmol) was added to a solution of 1-ethynylnaphthalene (0.043 g, 0.28 mmol) and 3 mL Et_3N in THF (30 mL) and stirred for 4 h. The crude solution was run over a silica plug, eluting **3** with a solvent mixture with $V_{hexanes}$:V_{EtOAc}:V_{THF}=89:10:1. The ensuing recrystallization from THF/MeOH yielded **3** as deep red, crystalline solid (52 mg, 0.048 mmol, 46% based on Ru). ESI-MS (*m/z*): [M+H]$^+$, 1094. ^{1}H NMR ($CDCl_3$): δ 8.59 (dd, *J*=7.9, 1.4 Hz, 2H), 7.71 (dd, *J*=6.9, 1.3 Hz, 2H), 7.51~7.32 (m, 22H), 7.10~7.03 (m, 8H), 3.42 (s, 24H). Visible spectra, λ_{max} / nm (ε / (L·mol^{-1}·cm^{-1})): 372sh (32 162), 391 (33 184), 508 (18 195), 681sh (1 791), 892 (3 214). IR (cm^{-1}): C≡C: 2 063 (s). Anal. Found (Calcd.) for $C_{60}H_{60}N_8O_1Ru_2$ (**3**·H_2O, %): C, 64.85 (64.85); H, 5.64 (5.44); N, 9.97 (10.08).

1.6 Preparation of 4

$Ru_2(DMBA)_4(NO_3)_2$ (0.085 g, 0.093 mmol) was added to a solution of 9-ethynylanthracene (0.055 g, 0.27 mmol) and 1.5 mL Et_2NH in THF (20 mL) and stirred 12 h. The crude solution was purified similarly to that of **3** to afford 50 mg of **4** (0.042 mmol, 45% based on Ru). ESI-MS (*m/z*): [M+H]$^+$,1195. ^{1}H NMR ($CDCl_3$): δ 8.88 (d, *J*=8.4 Hz, 4H), 7.93 (s, 2H), 7.86 (d, *J*=8.5 Hz, 4H), 7.51~7.30 (m, 20H), 7.13 (d, *J*=6.8 Hz, 8H), 3.55 (s, 24H). Visible spectra, λ_{max} / nm (ε / (L·mol^{-1}·cm^{-1})): 283sh (35 544), 289 (49 953), 502 (41 938), 699sh (1 785), 903 (2 291). IR (cm^{-1}): C≡C: 2045 (s). Anal. Found (Calcd.) for $C_{72}H_{73}N_8O_{2.5}Ru_2$ (**4**·1.5H_2O·THF, %): C, 66.97 (66.91); H, 5.76 (5.69); N, 8.53 (8.67).

CCDC: 1555598, **1**; 1555599, **2**; 1555609, **3**; 1555611, **4**.

2 Results and discussion

2.1 Syntheses

As shown in Scheme 1, compounds **1**~**4** were prepared from the direct reaction between $Ru_2(DMBA)_4(NO_3)_2$[29] and HC_2Ar in the presence of Et_3N/Et_2NH in satisfactory to very good yields after purification. Consistent with the previous studies of related

compounds, compounds **1**~**4** are diamagnetic, which facilitate their characterization using ^{1}H NMR. In addition, the purity of these compounds was also confirmed by combustion analysis.

2.2 Crystal structures

Molecular structures of compounds **1**~**4** have been determined using single crystal X-ray diffraction and structural plots are shown in Fig.1. While molecules **2**~**4** do not contain a crystallographic symmetry element, there is a C_2 axis passing through the midpoint of the Ru-Ru bond and relating two adjacent DMBA ligands in **1**. It is clear from Fig.1 that all compounds adopt the expected paddlewheel geometry with four equatorial bridging DMBA and two axial arylethynyl ligands. The Ru-Ru bond lengths are within a narrow range of 0.245 0~0.249 1 nm, which agrees with the values reported for other $Ru_2(DMBA)_4(C_2R)_2$ type compounds[2] and is consistent with the presence of a Ru-Ru single bond. The Ru-C bond lengths in **1**~**4** (0.196~0.201 nm) are also in agreement with the previous reports[2,33].

A notable structural feature of the $Ru_2(DMBA)_4(C_2Ar)_2$ type compounds is the significant distortion of the first coordination sphere of the Ru_2 core from an idealized paddlewheel structure (D_{4h}). The origin of such distortion is rooted in a second order Jahn-Teller effect, as originally proposed to rationalize the structures of the $Ru_2(DArF)_4(C_2Ph)_2$ type compounds (DArF =*N*,*N*′-diarylformamidinate)[34]. The structural distortion is typically reflected by (i) the large variation in Ru-N

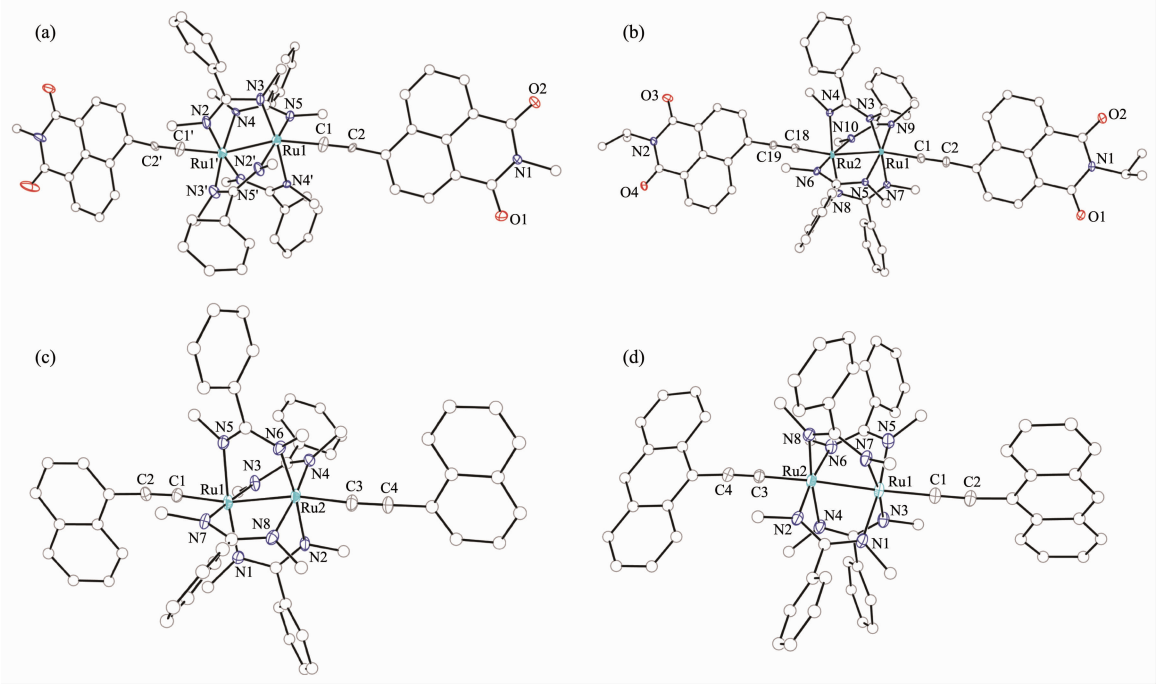

Hydrogen atoms were omitted for clarity

Fig.1 ORTEP plots of compounds **1** (a), **2** (b), **3** (c) and **4** (d) at 30% probability level

Table 1 Selected bond lengths (nm) and angles (°) for compounds 1~4*

			1		
Ru1-Ru1′	0.249 1(2)	Ru1-N3	0.201 0(16)	C1-C2	0.124(2)
Ru1-C1	0.201 0(17)	Ru1-N4	0.218 1(12)		
Ru1-N2	0.204 0(18)	Ru1-N5	0.199 7(17)		
Ru1′-Ru1-C1	162.5(5)	Ru1′-Ru1-N3	93.4(4)	Ru1′-Ru1-N5	93.9(4)
Ru1′-Ru1-N2	81.2(4)	Ru1′-Ru1-N4	79.2(4)		

Continued Table 1

			2		
Ru1-Ru2	0.245 67(4)	Ru1-N7	0.210 5(3)	Ru2-N10	0.206 5(3)
Ru1-C1	0.197 1(4)	Ru1-N9	0.199 6(3)	C1-C2	0.120 6(6)
Ru2-C18	0.195 8(4)	Ru2-N4	0.209 9(3)	C18-C19	0.121 4(6)
Ru1-N3	0.201 1(3)	Ru2-N6	0.200 5(3)		
Ru1-N5	0.208 3(3)	Ru2-N8	0.199 6(3)		
Ru2-Ru1-N3	91.24(9)	Ru1-Ru2-N4	81.62(9)	Ru2-Ru1-C1	167.74(12)
Ru2-Ru1-N5	82.59(8)	Ru1-Ru2-N6	90.49(9)	Ru1-Ru2-C18	167.44(12)
Ru2-Ru1-N7	81.12(9)	Ru1-Ru2-N8	92.12(9)		
Ru2-Ru1-N9	90.15(8)	Ru1-Ru2-N10	83.24(9)		
			3		
Ru1-Ru2	0.244 98(6)	Ru1-N5	0.211 8(4)	Ru2-N8	0.209 8(6)
Ru1-C1	0.196 1(6)	Ru1-N7	0.200 6(6)	C1-C2	0.121 3(9)
Ru2-C3	0.198 2(7)	Ru2-N2	0.208 1(5)	C3-C4	0.121 7(9)
Ru1-N1	0.199 0(5)	Ru2-N4	0.201 7(6)		
Ru1-N3	0.205 6(6)	Ru2-N6	0.200 8(5)		
Ru2-Ru1-N1	91.56(15)	Ru1-Ru2-N2	82.03(14)	Ru2-Ru1-C1	167.91(18)
Ru2-Ru1-N3	83.20(14)	Ru1-Ru2-N4	90.35(15)	Ru1-Ru2-C3	168.4(2)
Ru2-Ru1-N5	81.57(13)	Ru1-Ru2-N6	91.83(15)		
Ru2-Ru1-N7	90.99(15)	Ru1-Ru2-N8	81.91(15)		
			4		
Ru1-Ru2	0.245 06(3)	Ru1-N5	0.203 8(2)	Ru2-N8	0.204 1(2)
Ru1-C1	0.197 1(3)	Ru1-N7	0.206 3(2)	C1-C2	0.121 1(4)
Ru2-C3	0.196 3(2)	Ru2-N2	0.205 1(2)	C3-C4	0.121 2(4)
Ru1-N1	0.203 9(2)	Ru2-N4	0.206 1(2)		
Ru1-N3	0.203 8(2)	Ru2-N6	0.204 5(2)		
Ru2-Ru1-N1	86.87(6)	Ru1-Ru2-N2	86.08(6)	Ru2-Ru1-C1	177.8(3)
Ru2-Ru1-N3	87.68(6)	Ru1-Ru2-N4	84.84(6)	Ru1-Ru2-C3	176.7(2)
Ru2-Ru1-N5	85.90(6)	Ru1-Ru2-N6	86.70(6)		
Ru2-Ru1-N7	84.87(6)	Ru1-Ru2-N8	88.06(6)		

* There are two crystallographically independent molecules in compounds **1**~**3**; geometric parameters for only one of them are tabulated herein.

bond lengths, (ii) both acute and obtuse Ru-Ru-N angles, and (iii) significantly nonlinear Ru-Ru-C angles. These are clearly the case for the structures of **1**~**3**. However, the distortion is completely suppressed in **4**: Ru-N bond lengths are within a narrow range, Ru-Ru-N angles are all acute and Ru-Ru-C angles are fairly linear. We surmise that the steric effect of anthracene may be responsible for a more symmetric structure.

2.3 Vis-NIR spectroscopy and voltammetry

As noted earlier, all four compounds have a deep wine red color with a slight variation in hue. The Vis-NIR absorption spectra of **1**~**4** are shown in Fig.2, featuring a distinctive NIR band around *ca.* 880 nm that is responsible for the wine red color. This absorption is likely attributed to the $\pi^*(Ru_2)\rightarrow\delta^*(Ru_2)$ transition according to a prior TD-DFT analysis of related $Ru_2(DMBA)_4(C_2R)_2$ compounds[20]. The Vis

region is dominated by a very intense band with a transition energy depending on the nature of Ar. While the λ_{max} for Ar as both NAP^{me} (**1**) and NAP^{iso} (**2**) are 550 nm, the λ_{max} for Ar as Naphth (**3**) and Ant (**4**) are blue-shifted to 508 and 502 nm, respectively. This absorption may be assigned to the $\delta(Ru_2)+\pi(C\equiv C)\rightarrow\sigma^*$(Ru-C) transition based on the said TD-DFT study, which provides a ready rationale for the observed energy dependence on Ar. Electron donating Naphth and Ant destabilize σ^*(Ru-C) more significantly than electron withdrawing NAP^{me} and NAP^{iso}, which led to significantly wider optical gaps for **3** and **4**. The Vis spectra of both **1** and **2** also feature a shoulder at ca. 450 nm that is absent in the spectra of **3** and **4**, pointing to a possible NAP based transition. Also noteworthy is that while all four aryl ligands are strongly fluorescent, compounds **1**~**4** are non-emissive, reflecting the efficient quenching by the $Ru_2(DMBA)_4$ core.

$Ru_2(DMBA)_4(C_2R)_2$ type compounds often display rich electrochemical characteristics[20,26-27,33] and compounds **1**~**4** are no exception. As shown in Fig.3, their cyclic voltammograms (CV) all consist of two reversible one-electron couples, an oxidation (**A**) and a reduction (**B**), and both are Ru_2-based. It is also clear that the electrode potentials of compounds **1** and **2** are far more positive than those of the corresponding couples in **3** and **4**, reflecting the electron-deficient nature of NAP ligands. Since the oxidation and reduction potentials can be respectively correlated with the HOMO and LUMO energies[35-36], the electrochemical HOMO-LUMO gap (E_g) can be directly calculated from the difference between $E_{1/2}(A)$ and $E_{1/2}$ (**B**), and the values for **1**~**4** are listed in Table 2. Interestingly, the E_g remains fairly constant across the series despite the large variance in electrode potentials. Clearly, both the HOMO and LUMO are Ru_2-based, and the inductive ligand effects on their energies are about the same within the experimental errors.

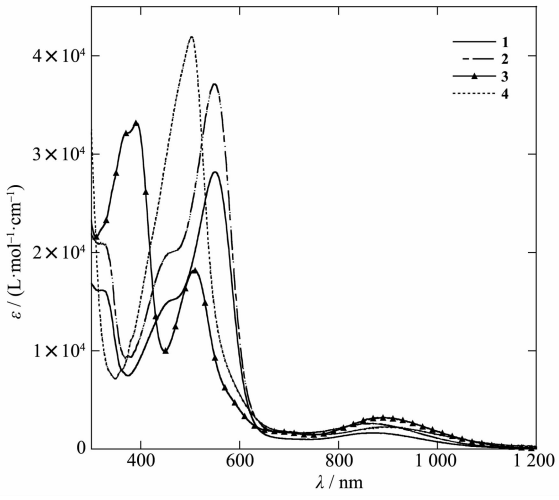

Fig.2 Vis-NIR spectra of compounds **1**~**4** recorded in THF solution

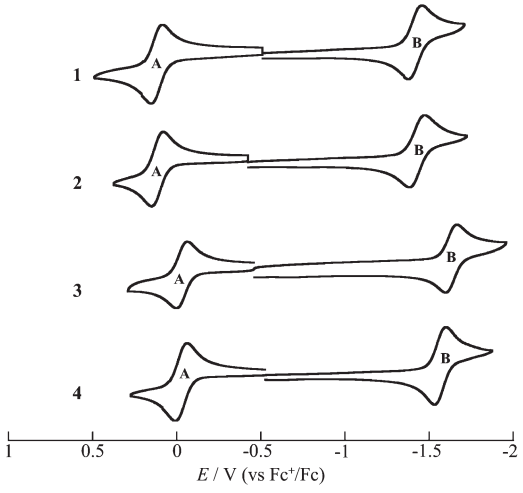

Fig.3 Cyclic voltammograms of compounds **1**~**4** recorded in 0.10 mol·L^{-1} THF solution of Bu_4NBF_4 at the scan rate of 100 mV·s^{-1}

Table 2 Electrode potentials of observed redox couples in $Ru_2(DMBA)_4(C_2Ar)_2$

Ar	$E_{1/2}$ (**A**) / V (ΔE_p / mV, i_{back} / $i_{forward}$)	$E_{1/2}$ (**B**) / V (ΔE_p / mV, i_{back} / $i_{forward}$)	E_g^* / V
NAP^{me} (**1**)	0.120 (68, 0.90)	−1.42 (73, 0.96)	1.54
NAP^{iso} (**2**)	0.120 (67, 0.92)	−1.43 (92, 0.92)	1.55
Naphth (**3**)	−0.03 (69, 0.97)	−1.63 (67, 0.97)	1.60
Ant (**4**)	−0.03 (68, 0.92)	−1.57 (76, 0.81)	1.54

*E_g=$E_{1/2}$(**A**)−$E_{1/2}$(**B**)

3 Conclusions

Four new $Ru_2(DMBA)_4(C_2Ar)_2$ compounds have been prepared and structurally characterized. While both the voltammetric responses and electronic absorption spectra are dominated by the Ru_2-centered processes, both the electrode potentials and excitation energies exhibit significant dependence on the arylethynyl ligands.

References:

[1] Paul F, Lapinte C. *Coord. Chem. Rev.*, **1998**,**178-180**:431-509

[2] Ren T. *Organometallics*, **2005**,**24**:4854-4870

[3] Costuas K, Rigaut S. *Dalton Trans.*, **2011**,**40**:5643-5658

[4] Blum A S, Ren T, Parish D A, et al. *J. Am. Chem. Soc.*, **2005**,**127**:10010-10011

[5] Meng F B, Hervault Y M, Norel L, et al. *Chem. Sci.*, **2012**,**3**:3113-3118

[6] ZHANG Xiang-Yi(张相宜), ZHENG Qi(郑启), QIAN Chen-Xi(钱晨熹), et al. *Chinese J. Inorg. Chem.*(无机化学学报), **2011**,**27**:1451-1464

[7] Wen H M, Yang Y, Zhou X S, et al. *Chem. Sci.*, **2013**,**4**:2471-2477

[8] Chen Z N, Zhao N, Fan Y, et al. *Coord. Chem. Rev.*, **2009**, **253**:1-20

[9] Yam V W-W. *Acc. Chem. Res.*, **2002**,**35**:555-563

[10]Wong W Y, Ho C L. *Acc. Chem. Res.*, **2010**,**43**:1246-1256

[11]Liu S H, Xia H P, Wen T B, et al. *Organometallics*, **2003**, **22**:737-743

[12]Liu S H, Hu Q Y, Xue P, et al. *Organometallics*, **2005**,**24**:769-772

[13]Kong D D, Xue L S, Jiang R, et al. *Chem. Eur. J.*, **2015**,**21**:9895-9904

[14]Ou Y P, Zhang J, Zhang F X, et al. *Dalton Trans.*, **2016**,**45**:6503-6516

[15]Xu L J, Zeng X C, Wang J Y, et al. *ACS Appl. Mater. Interfaces*, **2016**,**8**:20251-20257

[16]Zhang L Y, Xu L J, Wang J Y, et al. *Dalton Trans.*, **2017**, **46**:865-874

[17]Xu G L, Zou G, Ni Y H, et al. *J. Am. Chem. Soc.*, **2003**, **125**:10057-10065

[18]Cao Z, Xi B, Jodoin D S, et al. *J. Am. Chem. Soc.*, **2014**, **136**:12174-12183

[19]Wong K T, Lehn J M, Peng S M, et al. *Chem. Commun.*, **2000**:2259-2260

[20]Xu G L, Crutchley R J, DeRosa M C, et al. *J. Am. Chem. Soc.*, **2005**,**127**:13354-13363

[21]Zuo J L, Herdtweck E, de Biani F F, et al. *New J. Chem.*, **2002**,**26**:889-894

[22]Zuo J L, Herdtweck E, Kühn F E. *Dalton Trans.*, **2002**:1244-1246

[23]Mahapatro A K, Ying J, Ren T, et al. *Nano Lett.*, **2008**,**8**:2131-2136

[24]Zhu H, Pookpanratana S J, Bonevich J E, et al. *ACS Appl. Mater. Interfaces*, **2015**,**7**:27306-27313

[25]Ying J W, Cordova A, Ren T Y, et al. *Chem. Eur. J.*, **2007**, **13**:6874-6882

[26]Ying J W, Liu I P C, Xi B, et al. *Angew. Chem. Int. Ed.*, **2010**,**49**:954-957

[27]Cai X M, Zhang X Y, Savchenko J, et al. *Organometallics*, **2012**,**31**:8591-8597

[28]Wang C F, Zuo J L, Ying J W, et al. *Inorg. Chem.*, **2008**,**47**:9716-9722

[29]Xu G L, Jablonski C G, Ren T. *Inorg. Chim. Acta*, **2003**, **343**:387-390

[30]Chang N H, Mori H, Chen X C, et al. *Chem. Lett.*, **2013**,**42**:1257-1259

[31]Takahashi S, Kuriyama Y, Sonogashira K, et al. *Synthesis*, **1980**:627-630

[32]McAdam C J, Morgan J L, Murray R E, et al. *Aust. J. Chem.*, **2004**,**57**:525-530

[33]Xu G L, Campana C, Ren T. *Inorg. Chem.*, **2002**,**41**:3521-3527

[34]Lin C, Ren T, Valente E J, et al. *J. Chem. Soc., Dalton Trans.*, **1998**:571-576

[35]Ren T. *Coord. Chem. Rev.*, **1998**,**175**:43-58

[36]Loutfy R O, Loutfy R O. *Can. J. Chem.*, **1976**,**54**:1454-1463